



ELSEVIER

Physica C 364–365 (2001) 668–673

PHYSICA C

www.elsevier.com/locate/physc

# Topography and magnetoresistance in $\text{Nd}_{0.6}\text{Sr}_{0.4}\text{MnO}$ films

J.G. Lin<sup>a,\*</sup>, C.Y. Huang<sup>a</sup>, S.Y. Lin<sup>b</sup>, P.C. Kuo<sup>b</sup><sup>a</sup> Center for Condensed Matter Sciences, National Taiwan University, 1 Roosevelt Road, Sector 4, Taipei 106, Taiwan, ROC<sup>b</sup> Institute of Material Science and Engineering, National Taiwan University, Taipei 106, Taiwan, ROC

## Abstract

The highly textured  $\text{Nd}_{0.6}\text{Sr}_{0.4}\text{MnO}_3$  thin films with different thickness  $t$  were obtained. The maximum magnetoresistance (MR) ratio, defined as  $[R(0) - R(1.5 \text{ T})]/R(0)$  at the insulating- to metallic-phase transition temperature, was found to increase with decreasing  $t$ , reaching a value of 75% for  $t = 500 \text{ \AA}$ . However, when  $t$  was further decreased down to  $100 \text{ \AA}$ , the MR ratio was not significantly affected. In conjunction with our topographic results, we have attributed the saturation of MR ratio to the achieving of an optimized interface strain. © 2001 Elsevier Science B.V. All rights reserved.

PACS: 75.70; 68.55.-a; 75.30.k

Keywords: Thin film; Magnetoresistance;  $\text{Nd}_{0.6}\text{Sr}_{0.4}\text{MnO}_3$ 

## 1. Introduction

The discovery of colossal magnetoresistance (CMR) in manganese thin film La–Ca–Mn–O [1] has attracted much attention owing to its potential for the device applications. Nevertheless, the realization of the practical use of CMR films requires the improvement of their characterized properties, such as raising the Curie temperature ( $T_C$ ), and lowering the saturation field. According to the previous reports [2,3],  $\text{La}_{0.67}\text{Sr}_{0.33}\text{MnO}_3$  and  $\text{La}_{0.6}\text{Pb}_{0.4}\text{MnO}_3$  thin films already met the requirement from the aspect of their high  $T_C$ 's. The MR ratio (defined as  $[R(0) - R(H)]/R(0)$ ) at room temperature is 35% at 5 T for the  $\text{La}_{0.67}\text{Sr}_{0.33}\text{MnO}_2$  film and is 40% at 6 T for the  $\text{La}_{0.6}\text{Pb}_{0.4}\text{MnO}_3$  film.

However, to make devices out of these films, the good control of the film quality becomes very important, especially for different thickness [4] and with various growth processes [5]. The study [4] on the La–Ca–Mn–O epitaxial films revealed that the MR ratio strongly depends on the thickness ( $t$ ) of thin films. The MR ratio of  $\text{La}_{0.7}\text{Sr}_{0.3}\text{MnO}_3$  films increases with decreasing  $t$  from 2000 Å and reaches a maximum at  $t = 1000 \text{ \AA}$ . For  $t < 1000 \text{ \AA}$ , the MR ratio decreases with decreasing  $t$ . The authors proposed that there may be an optimal lattice strain for the high MR phenomenon or there may be some structural or chemical (e.g. oxygen stoichiometry) differences in very thin films that degrade the MR behavior. Later on, another group [6] suggested that the effect of lattice strain is a plausible interpretation, which also explains the thickness dependence of the magnetic microstructures of  $\text{La}_{0.7}\text{Sr}_{0.3}\text{MnO}_3$  films. Furthermore, a recent report [7] prevailed that the disorder existed in  $\text{La}_{0.7}\text{Ca}_{0.3}\text{MnO}_3$  thin film with  $t < 300 \text{ \AA}$ . It is,

\* Corresponding author. Tel.: +886-2-3630231; fax: +886-2-3655404.

E-mail addresses: jglin@ccms.ntu.edu.tw, jglin@phys.ntu.edu.tw (J.G. Lin).

then, interesting to learn whether the structural disorder is the main origin of the MR degradation or it is the intrinsic property having a strain-dependent MR ratio in the manganese thin films.

In an attempt to optimize a CMR thin film with high  $T_C$  and high MR ratio, and to understand the thickness dependence of MR ratio, we have sputtered four  $\text{Nd}_{0.6}\text{Sr}_{0.4}\text{MnO}_3$  thin films with different thickness and have studied their MR behavior. We have found that the MR ratio continuously increases with decreasing  $t$  from 1500, 1000, to 500 Å but stops increasing for further decreasing  $t$ . It seems that there indeed exists an optimum  $t$  for a maximum MR ratio. However, the optimum  $t$  we have found is much smaller than that was found in a previous report [4]. The difference between our result and that for La–Ca–Mn–O will be discussed in conjunction with other experimental evidence.

## 2. Experiments

Four  $\text{Nd}_{0.6}\text{Sr}_{0.4}\text{MnO}_3$  films with thickness of 1500, 1000, 500 and 100 Å were deposited on (100)  $\text{LaAlO}_3$  substrates at ambient temperature by a single-target magnetron sputtering system. The target with a nominal composition of  $\text{Nd}_{0.6}\text{Sr}_{0.4}\text{MnO}_3$  was prepared by a standard solid-state reaction from ultra high purity (99.99%) oxides and carbonates. The background pressure before sputtering is  $10^{-8}$  Torr and the sputtering pressure is 90 mTorr with  $\text{O}_2/\text{Ar} = 1/9$ . The temperature dependent resistivity was measured by using a standard four-point probe in a close cycle system and at the applied field up to 1.5 T. Temperature dependent magnetization was measured using a commercial SQUID magnetometer. The structures of these films were determined by the X-ray powder diffraction with a Scientag (X1) diffractometer (CuK radiation). The surface topography was examined by a atomic force microscopy (AFM).

## 3. Results and discussion

X-ray diffraction patterns of a 1500 Å film was shown in Fig. 1. The lowest pattern is for a

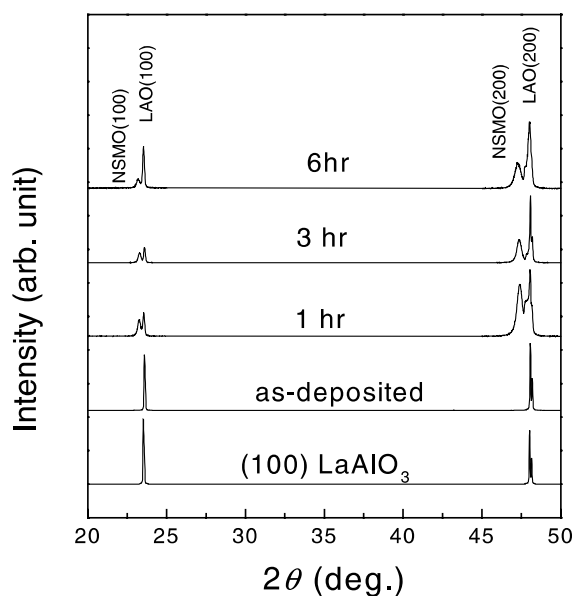


Fig. 1. X-ray data for a (100)  $\text{LaAlO}_3$  substrate (see the bottom pattern) and for  $\text{Nd}_{0.6}\text{Sr}_{0.4}\text{MnO}_3$  films with different annealing conditions.

$\text{LaAlO}_3$  substrate, the second one from the bottom is for an as-deposited film and the third to the fifth ones are for the films with 1–6 h annealing at 900°C in  $\text{O}_2$  atmosphere, respectively. It illustrates that the orthorhombic perovskite structure with  $c$ -axis perpendicular to the film surface forms after annealing in  $\text{O}_2$  for 1 h.

Based on the resistivity  $\rho$  data, the as-deposited film was an insulator. After annealing, it shows an insulator–metal transition. Fig. 2 indicates that  $\rho$  decreases first when annealing time increases from 1 to 3 h, then, increases with time increasing from 3 to 6 h. We attributed the increase of  $\rho$  with further annealing to the impurity scattering induced by the excess oxygen, and, hence, chose 3 h to be the optimal annealing time. We noted that although  $\rho$  changes with annealing time (see Fig. 2), the insulating to metal transition temperature  $T_p$  keeps nearly constant at  $\sim 240$  K for all three annealing conditions. The dashed lines in Fig. 2 represent the  $\rho$ – $T$  curve under the magnetic field of 1.5 T and were used to calculate the MR ratio according to the formula  $\text{MR} = [R(0) - R(1.5 \text{ T})]/R(0)$ . The corresponding MR ratio at

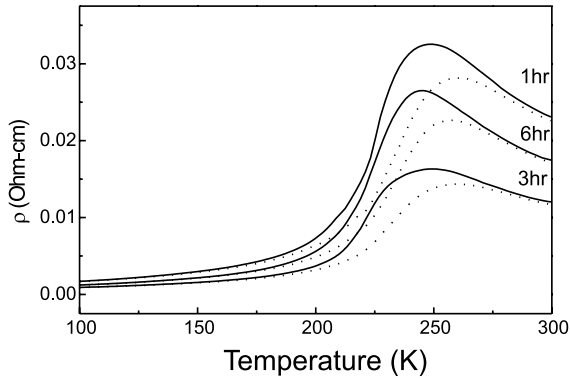


Fig. 2. Resistivity vs. temperature for a  $\text{Nd}_{0.6}\text{Sr}_{0.4}\text{MnO}_3$  film with 1500 Å thickness after being annealed for different time. Solid lines are the data measured at zero field and the dashed lines are the ones measured at 1.5 T.

240 K is 40%, 45%, and 43% with respect to the sample with 1, 3, and 6 h annealing, respectively. Compared with the MR result in  $\text{Nd}_{0.7}\text{Sr}_{0.3}\text{MnO}_3$  thick films [8], although a very high MR ratio, defined as  $\Delta R/R$  (6 T), was reported as  $10^6\%$ , it was obtained at a much higher field (6 T) and lower temperature (60 K). Using the same definition as ours for the MR ratio, their MR ratio is  $\sim 97\%$  at 6 T and at 60 K.

We also obtained that  $\rho$  increases with decreasing thickness from 1500, 1000, 500 to 100 Å; while  $T_p$  decreases with decreasing thickness. The values of  $T_p$  are consistent with  $T_C$  values determined from the magnetization vs. temperature data. The most dramatic change in both  $\rho$  and  $T_p$  occurs when  $t$  decreases from 500 to 100 Å.  $T_p$  decreases from 220 to 170 K while  $\rho$  increases by one order of magnitude, indicating that the strain effect is enhanced greatly in the film of 100 Å. Fig. 3 demonstrates the  $T$ -dependent MR ratio for four films. MR ratio at  $T_p$  are 45%, 55%, 75% and 75% for samples with  $t = 1500, 1000, 500$  and 100 Å, respectively. It is interesting to note that the MR ratio for film of 500 Å is roughly the same as that of 100 Å although their  $T_C$  and  $\rho$  are changed dramatically. This result of thickness dependent MR ratio is different from the report of Jin et al. [4] in which the optimum  $t$  was found to be 1000 Å in  $\text{La}_{0.67}\text{Ca}_{0.33}\text{MnO}_x$  for a maximum MR. For their samples with  $t = 500$  and 100 Å,  $\rho$  is

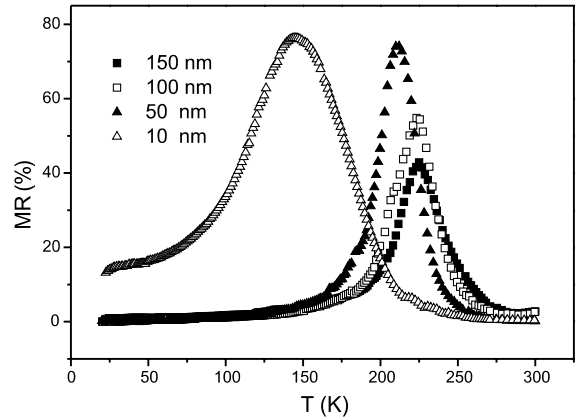


Fig. 3. MR ratio vs. temperature for  $\text{Nd}_{0.6}\text{Sr}_{0.4}\text{MnO}_3$  films with different thickness (■) 1500 Å; (□) 1000 Å; (○) 500 Å and (△) 100 Å.

very large and MR ratio drops by two orders of magnitude. The authors have attributed this optimal thickness effect to two possible reasons: (1) an optimal lattice strain for the high MR phenomenon or (2) some structural/chemical (e.g. oxygen stoichiometry) differences in very thin films.

The possibility of being structurally disordered for very thin films was evidenced in the  $\text{La}_{0.67}\text{Ca}_{0.33}\text{MnO}_x$  film with  $t < 300$  Å [7]. According to Ref. [7], the structural disorders for films with  $t < 300$  Å were observed from the high resolution HREM images and resulted into the separation of  $T_C$  and  $T_p$ . Since neither the microstructure nor the comparison of  $T_p$  and  $T_C$  was shown in Jin's report, it cannot be ruled out that the observed degradation of the MR ratio in Jin's films is due to the disorder presented in their films with  $t < 2000$  Å. However, for all our  $\text{Nd}_{0.6}\text{Sr}_{0.4}\text{MnO}_3$  films  $T_p$  coincides with  $T_C$ . Thus, the saturation of MR ratio at 500 Å in our films should not be attributed to the structural disorder. Instead, it mainly comes from the optimal strain effect.

According to the hypothesis that the thickness dependence of the MR ratio is related to the change in the lattice strains induced by the mismatch between the substrate and the film, the MR ratio would be affected by changing  $t$  only for films thinner than their relaxation thickness. And, the thinner the film is, the stronger the strain effect is.

For a  $\text{La}_{0.7}\text{Sr}_{0.3}\text{MnO}_x$  film on the (001)  $\text{LaAlO}_3$  substrate the mismatch is  $-2.4\%$  and its relaxation thickness is  $2500 \text{ \AA}$  [7]. For a  $\text{La}_{0.67}\text{Sr}_{0.33}\text{MnO}_x$  film on the  $\text{LaAlO}_3$  substrate the mismatch is  $\sim -2.0\%$  and its relaxation thickness is  $2000 \text{ \AA}$  [5]. For our  $\text{Nd}_{0.6}\text{Sr}_{0.4}\text{MnO}_3$  films the mismatch is  $\sim -1.6\%$ , we therefore expect the relaxation thickness to be around  $1500 \text{ \AA}$  for this system. Our observation that MR increases with decreasing  $t$  for  $t \leq 1500 \text{ \AA}$  agrees with this hypothesis. However, the strain effect does not explain the saturation of MR ratio for  $t \leq 500 \text{ \AA}$ .

We have related this problem to the thickness dependence of MFM images in  $\text{La}_{0.7}\text{Sr}_{0.3}\text{MnO}_x$  films. Kwon et al. reported [6] that the strain induced maze pattern appeared for  $360 < t \leq 1680 \text{ \AA}$  and disappears for  $t \leq 360 \text{ \AA}$ . It seems that when  $t$  is below a certain value, the strain does not affect the magnetic microstructure any more. Since the magnetic microstructures of films are mostly correlated with their topographic microstructures, we have investigated the thickness dependence of the

topographic structures in  $\text{Nd}_{0.6}\text{Sr}_{0.4}\text{MnO}_3$  films. Here, we describe the different features of their topography based on the AFM images. For  $t = 1500 \text{ \AA}$ , the film consists of in-plane oriented square layered islands of about  $50 \text{ nm}$  (see Fig. 4). For  $t = 1000 \text{ \AA}$ , the square islands develop into rectangular shapes (see Fig. 5). For  $t = 500 \text{ \AA}$ , the grain shapes become longitudinal and the boundaries between grains become blurred (see Fig. 6). Finally, at  $t = 100 \text{ \AA}$ , the film becomes a coalesced extended layer (see Fig. 7). Based on the topography result, the strain was less affective to the films with  $t = 1500\text{--}500 \text{ \AA}$ , because they are layer structure and the bonding between layers are not very strong. On the other hand, the film of  $t = 100 \text{ \AA}$  is an extended layer with some voids, which should experience the interface strain directly. The AFM result prompts us to believe that the saturation of the MR ratio in our films is closely related to an optimized strain.

In conclusion, we have obtained the highly textured  $\text{Nd}_{0.6}\text{Sr}_{0.4}\text{MnO}_3$  films with different thickness

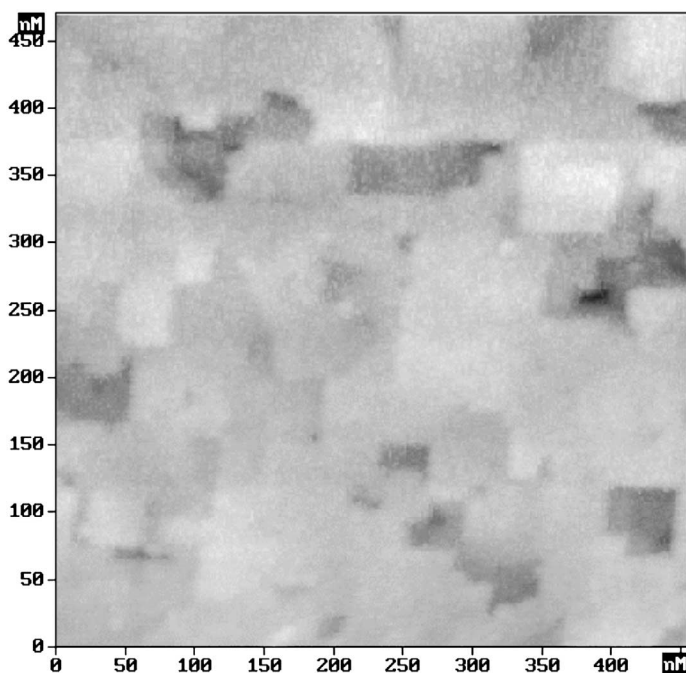


Fig. 4. Image of the AFM for a  $\text{Nd}_{0.6}\text{Sr}_{0.4}\text{MnO}_3$  film with  $1500 \text{ \AA}$  thickness.

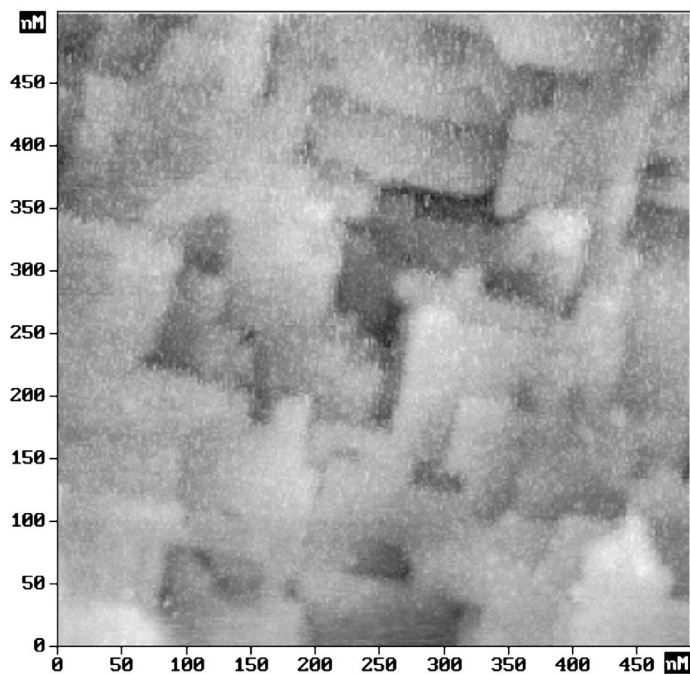


Fig. 5. Image of the AFM for a  $\text{Nd}_{0.6}\text{Sr}_{0.4}\text{MnO}_3$  film with 1000 Å thickness.

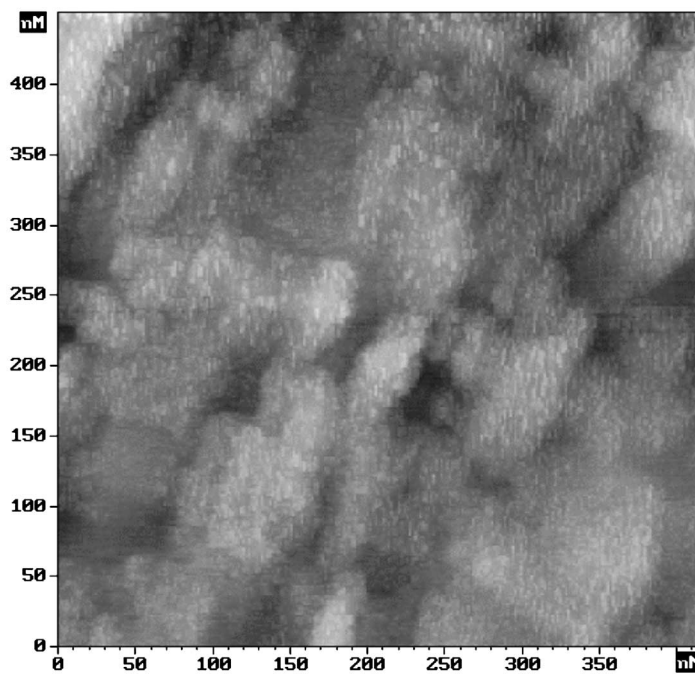


Fig. 6. Image of the AFM for a  $\text{Nd}_{0.6}\text{Sr}_{0.4}\text{MnO}_3$  film with 500 Å thickness.

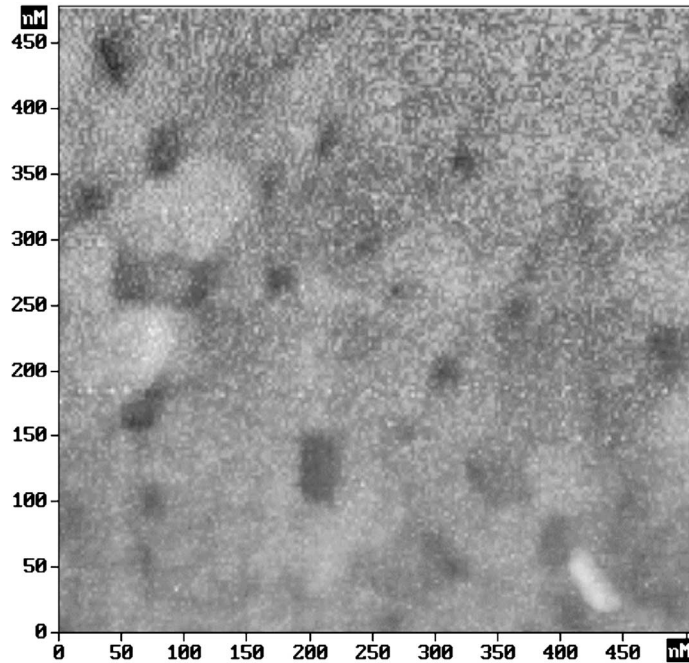


Fig. 7. Image of the AFM for a  $\text{Nd}_{0.6}\text{Sr}_{0.4}\text{MnO}_3$  film with 100 Å thickness.

$t$ , and have observed an increase of the MR ratio with decreasing  $t$  for  $500 \leq t \leq 1500$  Å. However, further decreasing of  $t$  affects only the  $M-I$  transition temperature and resistivity but not the MR ratio. In conjunction with the thickness dependence of AFM results, we propose that the saturation of the MR ratio in our  $\text{Nd}_{0.6}\text{Sr}_{0.4}\text{MnO}$  films could be due to the achieving of an optimized strain.

### Acknowledgements

J.G. Lin would like to thank Mr. D.H. Ngu for the AMF measurement. This work is supported in part by the National Science Council of the ROC under grant nos. NSC-89-2112-M-002-030 and NSC-89-2112-M-002-081.

### References

- [1] S. Jin, T.H. Tiefel, M. McCormack, R.A. Fastnacht, R. Ramesh, L.H. Chen, *Science* 64 (1994) 413.
- [2] H.L. Ju, C. Kwon, Q. Li, R.L. Greene, T. Venkatesan, *Appl. Phys. Lett.* 65 (1994) 2108.
- [3] S. Sundar Manoharan, N.Y. Vasanthacharya, M.S. Hegde, K.M. Satyalakshmi, V. Prasad, S.V. Subramanyam, *J. Appl. Phys.* 76 (1994) 3923.
- [4] S. Jin, T.H. Tiefel, M. McCormack, H.M. O'Bryan, L.H. Chen, R. Ramesh, D. Schurig, *Appl. Phys. Lett.* 67 (1995) 557.
- [5] M.E. Hawley, C.D. Adams, P.N. Arendt, E.L. Brosha, F.H. Garzon, R.J. Houlton, M.F. Hundley, R.H. Heffner, Q.X. Jia, J. Neumeier, X.D. Wu, *J. Cryst. Growth* 174 (1997) 455.
- [6] C. Kwon, M.C. Robson, K.-C. Kim, J.Y. Gu, S.E. Lofland, S.M. Bhagat, Z. Trajanovic, M. Rajeswari, T. Venkatesan, A.R. Kratz, R.D. Gomez, R. Ramesh, *J. Mag. Mag. Mater.* 172 (1997) 229.
- [7] J. Aarts, S. Freisem, R. Hendriks, H.W. Zandbergen, *Appl. Phys. Lett.* 72 (1998) 2975.
- [8] G.C. Xiong, Q. Li, H.L. Ju, S.N. Mao, L. Senpati, X.X. Xi, R.L. Greene, *Appl. Phys. Lett.* 66 (1995) 1427.